

OPEN ACCESS

Right sneutrino dark matter and a monochromatic photon line

To cite this article: Arindam Chatterjee *et al* JCAP07(2014)023

View the [article online](#) for updates and enhancements.

Related content

- [WIMPs at the galactic center](#)
Prateek Agrawal, Brian Batell, Patrick J. Fox *et al.*
- [Minimal semi-annihilating \$\tilde{\nu}\$ scalar dark matter](#)
Geneviève Bélanger, Kristjan Kannike, Alexander Pukhov *et al.*
- [Low-mass right-handed sneutrino dark matter: SuperCDMS and LUX constraints and the Galactic Centre gamma-ray excess](#)
D.G. Cerdeño, M. Peiró and S. Robles

Recent citations

- [Dark matter candidates in the NMSSM with RH neutrino superfields](#)
Daniel E. López-Fogliani *et al*
- [Bayesian analysis of sneutrino dark matter in the NMSSM with a type-I seesaw mechanism](#)
Junjie Cao *et al*
- [Natural SUSY at LHC with right-sneutrino LSP](#)
Arindam Chatterjee *et al*



IOP ebooksTM

Bringing together innovative digital publishing with leading authors from the global scientific community.

Start exploring the collection—download the first chapter of every title for free.

Right sneutrino dark matter and a monochromatic photon line

Arindam Chatterjee,^a Debottam Das,^b Biswarup Mukhopadhyaya^a
and Santosh Kumar Rai^a

^aRegional Centre for Accelerator-based Particle Physics, Harish-Chandra Research Institute,
Chhatnag Road, Jhusi, Allahabad 211019, India

^bInstitut für Theoretische Physik und Astrophysik, Universität Würzburg,
Am Hubland, 97074 Würzburg, Germany

E-mail: arindam@hri.res.in, debottam.das@physik.uni-wuerzburg.de,
biswarup@hri.res.in, skrai@hri.res.in

Received January 21, 2014

Revised April 26, 2014

Accepted June 16, 2014

Published July 11, 2014

Abstract. The inclusion of right-chiral sneutrino superfields is a rather straight forward addition to a supersymmetric scenario. A neutral scalar with a substantial right sneutrino component is often a favoured dark matter candidate in such cases. In this context, we focus on the tentative signal in the form of a monochromatic photon, which may arise from dark matter annihilation and has drawn some attention in recent times. We study the prospect of such a right sneutrino dark matter candidate in the contexts of both MSSM and NMSSM extended with right sneutrino superfields, with special reference to the Fermi-LAT data.

Keywords: supersymmetry and cosmology, dark matter theory, particle physics - cosmology connection

ArXiv ePrint: [1401.2527](https://arxiv.org/abs/1401.2527)



Contents

1	Introduction	1
2	Breit-Wigner resonance: effect of threshold	2
3	Photon signal with $\tilde{\nu}_R$ dark matter	5
3.1	$\tilde{\nu}_R$ and the MSSM	6
3.2	$\tilde{\nu}_R$ and the NMSSM	7
3.2.1	ϕ_1/σ_1 dark matter	10
3.2.2	Degenerate ϕ_1 - σ_1 dark matter	12
3.2.3	Constraints from direct detection	14
4	Summary and Conclusions	15

1 Introduction

Various observations ranging from galactic rotation curves to the observed anisotropy in the cosmic microwave background radiation, have strengthened our belief in a substantial cold Dark Matter (DM) component of the universe. It is therefore hardly surprising that, side by side with direct searches, all indirect evidences of dark matter are also of great interest.

Analyses of the publicly available Fermi-LAT [1] data found a tentative hint through an observation of a γ -ray line at ~ 130 GeV coming from the vicinity of the galactic center [2–5]. In ref. [3] it was shown that a possible explanation for such a γ -ray line could be via DM pair annihilations into two photons, with a DM mass of $129.8 \pm 2.4_{-13}^{+7}$ GeV and annihilation cross-section $\langle\sigma v\rangle_{\gamma\gamma} = (1.27 \pm 0.32_{-0.28}^{+0.18}) \times 10^{-27} \text{cm}^3 \text{s}^{-1}$ [4–11]. Moreover, there is a faint indication (1.4σ) of two lines which can be extracted from the Fermi data, one at ~ 130 GeV and a weaker one at ~ 114 GeV [5, 12]. Such a pair of lines can be naturally explained by a DM particle of mass ~ 130 GeV annihilating into $\gamma\gamma$ and γZ with a relative annihilation cross-section $\langle\sigma v\rangle_{\gamma Z}/\langle\sigma v\rangle_{\gamma\gamma} = 0.66_{-0.48}^{+0.71}$ [13].

In ref. [14], this line feature was found to shift to ~ 133 GeV, obtained using reprocessed data. In any case, the observation points rather clearly towards a line in the range 130–135 GeV, which is unlikely to be explained by astrophysical considerations [16, 17].

Following reference [3], various models have been proposed to explain the monochromatic feature of the γ -ray, see e.g. [18–52]. Most models are further constrained from the continuum flux of photons arising from annihilations of the DM into W and Z bosons and the Standard Model (SM) fermions [24, 43–46]. Supersymmetric (SUSY) theories with a viable cold DM candidate have been well studied in this context. However it is found that within the minimalistic versions where the lightest neutralino is the DM candidate, it is very difficult to accommodate the γ -ray line signal. We can summarize the shortcomings as follows:

- In the minimal version, *viz.* the Minimal Supersymmetric Standard Model (MSSM), it is difficult to obtain the large annihilation cross-section of neutralino pairs into photons $\langle\sigma v\rangle_{\gamma\gamma}$ [53], while satisfying constraints imposed by the thermal relic density and large continuum flux [23] data.

- In the Next-to-Minimal Supersymmetric Standard Model (NMSSM), which addresses the μ -problem in MSSM, one can accommodate the large annihilation cross-section of the neutralino pairs into photons by exploiting the *very* singlet like CP-odd Higgs boson resonance [41, 42, 54, 55]. However, the parameter space is tightly constrained by the direct searches for the DM, most importantly by the data from XENON100 and LUX [56, 57]. It is however observed that in a specific region of the parameter space, where $\mu_{\text{eff}} < 0$, constraints from direct detection can be relaxed by an order, in compliance with the bound from XENON100 [47].

In addition, a 130–135 GeV photon signal can be produced both in the the MSSM and the NMSSM through internal bremsstrahlung [49, 58], although a significant boost factor is required [49] in the latter scenario.

In this work we study the feasibility of a new DM candidate, *viz.* a right-chiral sneutrino, $\tilde{\nu}_R$ (with some degree of mixing with a left-chiral one), as the candidate for producing the photon line. The simplest way to accommodate non-zero (Dirac) neutrino masses in SUSY models is by introducing a right-handed singlet neutrino. This would entail addition of right-chiral neutrino superfields in the MSSM.¹ In addition we ensure that the thermal relic density is in agreement with WMAP data [59] and also satisfies constraints from DM-nucleus scattering [56, 57]. Thanks to their singlet nature, the right-handed sneutrinos ($\tilde{\nu}_R$), acting as cold DM candidates [60–63] in the MSSM, can account for all tentative evidences of DM we have so far. A sizeable volume of work has also taken place on the LHCs signals of (right) sneutrino DM [64–67], and also on the related scenarios carrying implications on different aspects of phenomenology [68–72]. However, as we will discuss, a $\tilde{\nu}_R$ DM with mass of about 133 GeV, that can produce $\langle\sigma v\rangle_{\gamma\gamma} \sim 1.2 \times 10^{-27}$, falls short in accounting for all the continuum constraints.

To get around this difficulty, we consider a similar scenario in the Next-to-Minimal Supersymmetric Standard Model ($\tilde{\nu}_R$ NMSSM) with a scale invariant superpotential, assuming a $\tilde{\nu}_R$ type DM. Notably, $\tilde{\nu}_R$ can naturally acquire a Majorana mass term of $\mathcal{O}(1)$ TeV. In addition to contributing neutrino masses and mixings [73, 74], $\tilde{\nu}_R$ DM in the NMSSM may have rich phenomenology as discussed in ref: [75–78]. As will be discussed in detail, in this case, one can even evade the continuum constraints when considering resonant annihilation mediated via a singlet-like Higgs boson. Additionally, the constraints from XENON100 and LUX on the spin-independent direct detection cross-section can also be satisfied.

This paper is organized as follows: in section 2 we discuss resonant annihilation of DM; following which, in section 3, we explore the possibility of explaining the observed γ signal with $\tilde{\nu}_R$ DM in the MSSM and the NMSSM. Finally, we summarize in section 4.

2 Breit-Wigner resonance: effect of threshold

The pair annihilation of $\tilde{\nu}_R$ into two photons can proceed via a dominantly singlet/doublet like CP-odd (CP-even) Higgs A (H) in the s-channel. Before getting into specific models, we first discuss the annihilation of a spin-0 dark matter particle ($\tilde{\nu}_R$ in our context) with mass m , mediated via a spin-0 particle of mass M near the resonance. DM annihilations near resonances and thresholds have been previously studied [79–81]. Our discussion closely follows [80, 81].

¹In the standard seesaw extensions of MSSM, Majorana mass scale for the right handed neutrino superfields is very close the gauge coupling unification scale ($M_G \sim 10^{16}$ GeV) which makes right handed sneutrinos very massive (close to M_G), thus not suitable for electro-weak scale dark matter candidate.

The cross-section of an s-channel scattering process, near the resonance, is given by,

$$\sigma = \frac{32\pi}{4E_1 E_2 v \overline{\beta}_i} \frac{M^2 \Gamma^2}{(s - M^2)^2 + M^2 \Gamma^2} B_i B_f, \quad (2.1)$$

where $\overline{\beta}_i = \sqrt{1 - \frac{4m^2}{M^2}}$; B_i and B_f are the branching fractions of the intermediate particle into the initial and final channels respectively and Γ is the total decay width of the same; E_1 and E_2 are the energies of the two annihilating particles; $s = (p_1 + p_2)^2$ where p_1 and p_2 represent the four-momenta of the two annihilating particles. In the thermal averaging of σv , in the context of DM, the Møller velocity (v) is used [79]. However, in the rest frame of one of the annihilating particles, and also in the center of momentum (CM) frame, the Møller velocity is reduced to the relative velocity of these particles. Following ref. [80], to quantify the resonance, an auxiliary parameter δ is introduced, such that,

$$M^2 = 4m^2(1 - \delta). \quad (2.2)$$

Since, in the present context, the annihilating particles in resonance are non-relativistic, $|\delta| \ll 1$ is assumed. Note that for $\delta < 0$, a physical pole ($s = M^2$) is encountered when $v \simeq 2\sqrt{|\delta|}$ (in the CM frame, where v denotes the magnitude of the relative velocity of the annihilating particles); while, for $\delta > 0$, a physical pole is never encountered. In the former situation B_i , B_f are well-defined, consequently eq. (2.1) holds good in this region. However, in the latter ($\delta > 0$), the intermediate particle can no longer decay into two dark matter particles; consequently B_i and $\overline{\beta}_i$ are unphysical (imaginary numbers). However, $B_i/\overline{\beta}_i$ remains well-defined. In this case, eq. (2.1) can also be expressed as,

$$\sigma = \frac{2|C|^2}{4E_1 E_2 v} \frac{M\Gamma}{(s - M^2)^2 + M^2 \Gamma^2} B_f, \quad (2.3)$$

where, C denotes the coupling between dark matter particles and the mediating particle which in our context are $\tilde{\nu}_R$ and the CP-even or CP-odd Higgs respectively. In the CM frame, with non-relativistic dark matter particles ($v \ll 1$), we have $s \equiv 4m^2(1 + v^2/4)$. Eq. 2.1, then, reduces to [80],

$$\sigma v = \frac{32\pi}{M^2} \frac{\gamma^2 B_f}{(\delta + v^2/4)^2 + \gamma^2} \left(\frac{B_i}{\overline{\beta}_i} \right), \quad (2.4)$$

where $\gamma = \Gamma/M$.

In the limit of narrow width resonance $\gamma \ll 1$ while for $\max(|\delta|, \gamma) < v \ll 1$ the denominator of eq. (2.4) receives dominant contribution from v^2 , and thus σv is enhanced as v decreases. This behavior continues until $v \lesssim \max(|\delta|, \gamma)$. Finally, for $v \ll \max(|\delta|, \gamma)$, σv becomes insensitive to v , and is then determined only by δ and γ . On the contrary, in case of broad width resonance ($\gamma \gg 1$), with $\gamma \gg \max(|\delta|, v^2/4)$ and $v \ll 1$, γ^2 dominates in the denominator, and thus $\gamma^2/((\delta + v^2/4)^2 + \gamma^2) \simeq 1$.

Since DM annihilation into $\gamma\gamma$, in our case, is a loop-suppressed process, the required $\langle \sigma(\tilde{\nu}_R \tilde{\nu}_R \rightarrow \gamma\gamma)v \rangle \simeq 10^{-27} \text{ cm}^3 \text{ s}^{-1}$ apparently leads to a larger $\langle \sigma_{\text{ann}} v \rangle$, where σ_{ann} denotes the total annihilation cross-section of the DM into the SM particles. As all the tree-level processes are mediated by the same intermediate state (at resonance), it leads to a much lower thermal relic abundance. We therefore now discuss about how we achieve the required cross-section $\langle \sigma v \rangle$ for the γ signal, as well as the correct relic abundance.

- In the context of the γ signal, $\langle\sigma v\rangle$ annihilation cross-section needs to be evaluated at late times, i.e. typically when $v_{rel} \sim 0.001$. Thus, in eq. (2.4), with $|\delta| \sim \mathcal{O}(10^{-2})$, v can be ignored in the denominator. As we shall discuss in the next section, by suitably choosing the coupling C (eq. (2.3)) along with δ, γ , it is possible to achieve the required cross-section in the $\tilde{\nu}_R$ NMSSM.
- During freeze-out, away from a pole, the typical velocity of cold DM is about 0.3. Here, by freeze-out, we mean when $(n - n_{eq}) \simeq n_{eq}$; n and n_{eq} represent the DM density at a given time/temperature and the equilibrium value of the same respectively. Let the corresponding freeze-out temperature be denoted by T_f .² Since after freeze-out (in the absence of a pole) annihilations do not affect the relic abundance of DM significantly, the abundance at T_f usually provides a good estimate of relic abundance. Since DM is non-relativistic at freeze-out, the thermal abundance at T_f is exponentially suppressed by a factor $x_f = \frac{m}{T_f}$. The situation is different for the two regions in the vicinity of the pole, namely when $\delta > 0$ or $\delta < 0$. We discuss their characteristic features below:

□ For $\delta > 0$ we always have $s > M^2$ and therefore the annihilation processes will never hit the physical pole. In the region $v^2 > 4 \max(\delta, \gamma)$, the cross-section σ is dominated by γ/v^2 . Thus, $\langle\sigma v\rangle$, at a temperature $T \sim mv_0^2$ where $v_0^2 \gg \max(\delta, \gamma)$, is determined by γ/v_0^2 . At such large v_0 , $s > M^2$, and thus annihilations dominantly occur further away from the pole leading to suppressed cross-sections similar to the other annihilation channels (if allowed) which are not mediated via the resonance. However, as T , and therefore v_0 , decreases, the DM annihilation would be closer to the resonance and tend to have a larger $\langle\sigma v\rangle$, and thus, does not decouple. Consequently the DM can continue to annihilate through these channels until $v_0^2 < 4 \max(\delta, \gamma)$. After that, the corresponding σ does not change any more, and, assuming that these are the only annihilation channels, the relic density would then be determined by only δ and γ [80].

□ For $\delta < 0$, the pole is physical, i.e. $s = M^2$ can be achieved in the early Universe. Therefore, unlike the previous case, at $s = M^2$ or $v^2 \simeq 4|\delta|$, σ is very large. At high temperatures, $T \sim m|\delta|$, $\langle\sigma v\rangle$ is large, and then decreases with T . In the early Universe, at such high temperature, this leads to a large thermally averaged cross-section, especially when compared to the $\delta > 0$ case with similar couplings. It was shown in ref. [80] that the relic density remains similar to a scenario where DM has a similar annihilation cross-section even without the resonance. For smaller values of $|\delta|$ and γ a large boost factor (defined as $\frac{\langle\sigma v\rangle|_{T \rightarrow 0}}{\langle\sigma v\rangle|_{T \sim T_f}}$) can be obtained in this case too [81].

- The annihilation cross-section and therefore the time of freeze-out, while a little away from the pole, also has a moderate dependence on the coupling C (see eq. (2.3)). When $\delta > 0$, for large v_0 (in the early Universe), such that $v_0^2 \gtrsim 4 \max(\delta, \gamma)$ the contribution from the resonant annihilation can be small. The resonant channel decouples much late (i.e. when $\Gamma \simeq H$, where Γ and H denote the interaction rate with the thermal soup and the Hubble expansion rate respectively) as its contribution continues to increase until $v_0^2 \lesssim 4 \max(\delta, \gamma)$. But this late decoupling does not lead to exponential suppression (by $x_D = \frac{m}{T_D}$, where T_D is the decoupling temperature) to the relic density. On the

²We have used `micrOMEGAs` to obtain the freeze-out temperature, and also the relic abundance. Note that, `micrOMEGAs` uses $n(T_f) = 2.5 n_{eq}(T_f)$ to estimate the freeze-out temperature T_f [82–84].

other hand, for $\delta < 0$, resonant annihilation at high v_0 (at early times) leads to larger thermally averaged annihilation cross-section for similar values of the coupling C . This, in turn, results in late freeze-out and a lower relic abundance [80]. As we will elaborate in the next section, for our benchmark points, we will be able to obtain large relic in the $\delta > 0$ scenario. Similarly, as the DM annihilations into two photons also happens at late time, it is possible to obtain the required $\langle\sigma v\rangle_{\gamma\gamma}$ too.

3 Photon signal with $\tilde{\nu}_R$ dark matter

In the following, we discuss the different avenues of indirect detections for a relatively light $\tilde{\nu}_R$ dark matter focusing on the γ ray line observed at $E_\gamma \sim 130/135$ GeV. As mentioned earlier, we extend the MSSM and the NMSSM with three generations of right handed neutrino superfields ($\tilde{\nu}_R^c$). Assuming that the $\tilde{\nu}_R^c$ is the lightest SUSY particle (LSP) in the supersymmetric particle spectrum, we enforce that the following phenomenological constraints always hold.

- A relic density complying with the WMAP bound $\Omega h^2 = 0.1120 \pm 0.011$ [59] (with 2σ error bars).
- A SM-like Higgs boson with $M_{H_{SM}} = 124\text{--}127$ GeV.
- Constraints from B-physics, which have little impact for our choice of $\tan\beta$, are considered. These include constraints from $b \rightarrow s\gamma$ and $B_s \rightarrow \mu^+\mu^-$ which we have estimated using SPheno [91, 92].
- Upper bounds on annihilation cross sections into W^+W^- , ZZ , $b\bar{b}$ and $\tau\bar{\tau}$ channels from the Fermi LAT collaboration [85, 86], as well as bounds from PAMELA on the anti-proton flux [87].

For exact calculation of the sneutrino mass and mixing matrices as well as two-loop renormalization group equations (RGEs) for all SUSY parameters, we have used the publicly available code called SARAH [88–90]. These RGEs are then implemented in the software package SPheno [91, 92] for numerical evaluation of all physical parameters and phenomenological constraints. For computation of relic density, all indirect detection cross-sections and fluxes, we implement SARAH generated CalcHEP [93] model files into micrOMEGAs [82–84]. We however calculate the cross-section for the photon line $\langle\sigma v\rangle_{\gamma\gamma}$ signal with our own mathematica code based on refs. [80, 81]. We ignore the contribution of $\langle\sigma v\rangle_{\gamma\gamma}$ in the relic density computation.

In both the models that we have considered, we scan the parameter space while keeping the soft SUSY breaking terms in the following preferred ranges.

- Squark masses of 2–3 TeV are assumed to alleviate LHC constraints from direct SUSY searches. The latter choice also helps to enhance the lightest Higgs boson mass irrespective of the choice of $\tan\beta$. Similarly, gluino masses (M_G) is fixed around ~ 2 TeV. The slepton masses are assumed to be around 300 GeV to have consistent spectra with muon anomalous magnetic moment.
- Trilinear soft susy breaking terms $T_t = -3$ TeV and $T_b = -1.0$ TeV (scaled with the Yukawa couplings).

- We use $m_{\tilde{\nu}_R}^2$ as free parameter. Similarly, the couplings y_ν and T_ν for $\nu_l - \nu_R$ and $\tilde{\nu}_l - \tilde{\nu}_R$ are assumed flavor diagonal. In the present context, we refrain from exact calculation of neutrino masses and mixing angles.
- $\mu \sim \pm(200-300)$ GeV is assumed.
- We have used the top quark pole mass $m_{\text{top}} = 173.1$ GeV.

3.1 $\tilde{\nu}_R$ and the MSSM

In this section, we discuss the status of $\tilde{\nu}_R^c$ dark matter in the (R-parity conserving) MSSM with three generations of right-handed (s)neutrinos. The neutrino masses arise from the Yukawa interaction only (*purely Dirac-type*) and can be obtained from the following superpotential:

$$W = W_{\text{MSSM}} + y_\nu \hat{H}_u \cdot \hat{L} \hat{\nu}_R^c, \quad (3.1)$$

where W_{MSSM} denotes the MSSM superpotential; \hat{H}_u , \hat{L} and $\hat{\nu}_R^c$ represents the up-type Higgs, lepton doublet and right-handed neutrino superfields respectively. For simplicity, we consider all mass and coupling parameters to be real and suppress flavor indices for neutrino families. Assuming soft-supersymmetry breaking, as in the MSSM, the soft-breaking scalar potential becomes,

$$V_{\text{soft}} = V_{\text{MSSM}} + (T_\nu H_u \cdot \tilde{L} \tilde{\nu}_R^c + \text{h.c.}) + m_{\tilde{\nu}_R}^2 |\tilde{\nu}_R^c|^2, \quad (3.2)$$

where V_{MSSM} denotes the soft-supersymmetry breaking terms in the MSSM and soft trilinear coupling is given by $T_\nu \equiv T_{\nu\alpha} y_{\nu\alpha}$, where α denotes the generation index. Neutrino masses can be expressed as,

$$m_\nu = y_\nu \langle H_u^0 \rangle = y_\nu \frac{v}{\sqrt{2}} \sin \beta \quad (3.3)$$

where $v \simeq 246$ GeV is the vacuum expectation value (VEV) of the standard-model -like Higgs boson, and $\tan \beta = \langle H_u^0 \rangle / \langle H_d^0 \rangle$. Clearly, neutrino masses ($m_\nu \sim 0.1$ eV) put constraints on the size of the neutrino Yukawa couplings $y_\nu \sim \mathcal{O}(10^{-12})$. Ignoring flavor mixing in the $\tilde{\nu}$ sector³ the (2×2) mass matrix for $\tilde{\nu}_\alpha$ for any flavor α , can be written as,

$$m_{\tilde{\nu}_\alpha}^2 = \begin{pmatrix} m^{\alpha 2} & \frac{1}{\sqrt{2}} \left(-v_d \mu y_{\nu_\alpha}^* + v_u T_{\nu_\alpha}^* \right) \\ \frac{1}{\sqrt{2}} \left(-v_d \mu^* y_{\nu_\alpha} + v_u T_{\nu_\alpha} \right) & \frac{1}{2} v_u^2 |y_{\nu_\alpha}|^2 + m_{\tilde{\nu}_{R\alpha}}^2 \end{pmatrix} \quad (3.4)$$

with

$$m^{\alpha 2} = \frac{1}{8} \left(4v_u^2 |y_{\nu_\alpha}|^2 + 8m_{\tilde{l}_\alpha}^2 + (g_1^2 + g_2^2) (-v_u^2 + v_d^2) \right), \quad (3.5)$$

where $m_{\tilde{l}_\alpha}$ is the soft breaking term for \tilde{l}_α . The lightest sneutrino mass eigenstates $\tilde{\nu}_R^1$, as obtained after diagonalization of $\tilde{\nu}_\alpha$, can be a valid candidate for DM. Moreover, such a $\tilde{\nu}_R^1$ can also produce viable photon signal $\langle \sigma v \rangle_{\gamma\gamma, \gamma Z} \sim 10^{-27} \text{ cm}^3 \text{ s}^{-1}$, through the resonant annihilations via heavier CP-even (H_2) or CP-odd Higgs boson (A). Note that the resonant annihilation through CP-odd Higgs boson A can only take place if T_{ν_α} is complex, as otherwise the coupling among $A \tilde{\nu}_R^1 \tilde{\nu}_R^{1*}$ vanishes. The CP-odd Higgs resonance avoids stringent

³Although flavor violation cannot be ignored in the ν sector, in $\tilde{\nu}$ sector, it is only induced through terms proportional to y_ν , assuming the soft-breaking terms to be flavor conserving. Since y_ν is $\mathcal{O}(10^{-12})$, such effects are very small and do not affect our results.

constraints on $\langle\sigma v\rangle_{W^+W^-,ZZ}$ coming from continuum fluxes of gamma rays.⁴ We found that it requires large values of $\mathcal{I}m(T_{\nu_\alpha})$ to obtain the desired cross-section for the di-photon final state. However, a dominantly CP-odd Higgs resonance falls short in accounting for the desired thermal relic abundance; and, more importantly, the viable parameter space has been ruled out by constraints from the continuum spectrum of γ rays. In particular, we found that annihilation cross-sections to the following final states are somewhat above the upper limits set by the Fermi-LAT for a NFW halo profile [38, 46], *viz.* (i) $\langle\sigma v\rangle(\tilde{\nu}_R^1\tilde{\nu}_R^1 \rightarrow b\bar{b}) \sim 10^{-23}\text{cm}^3\text{s}^{-1}$ and (ii) $\langle\sigma v\rangle(\tilde{\nu}_R^1\tilde{\nu}_R^1 \rightarrow ZH) \sim 10^{-23}\text{cm}^3\text{s}^{-1}$.

Also, a significant left-right mixing in the lightest sneutrino states, which enhance the photon signal, is tightly constrained from the direct DM searches. Thus, in this extension of the MSSM, although $\tilde{\nu}_R^1$ is a viable DM candidate, achieving large $\langle\sigma v\rangle_{\gamma\gamma}$ seems to be incompatible with other constraints on DM.

3.2 $\tilde{\nu}_R$ and the NMSSM

Next we consider a similar extension of the scale invariant NMSSM, with three generations of right-handed neutrino superfields. The new superpotential becomes

$$W = W_{\text{MSSM}} + \lambda\hat{S}\hat{H}_u \cdot \hat{H}_d + \frac{\kappa}{3}\hat{S}^3 + y_\nu \hat{H}_u \cdot \hat{L} \hat{\nu}_R^c + \frac{y_r}{2} \hat{S} \hat{\nu}_R^c \hat{\nu}_R^c, \quad (3.6)$$

where W_{MSSM} denotes the MSSM superpotential without the μ term. The \hat{S} denotes the singlet superfield that already appears in the NMSSM. When the scalar component of \hat{S} gets a VEV of the order of electro-weak scale, μ term of correct size would be generated. Similarly, the right handed neutrinos also acquire an effective Majorana mass around the electro-weak values as long as the dimensionless coupling y_r is order one [73]. At the tree level the (3×3) light neutrino mass matrix, that arises via the seesaw mechanism, has a very well-known structure given by,

$$m_\nu^{\text{tree}} = -m_D M_R^{-1} m_D^T, \quad (3.7)$$

Unlike MSSM, here $y_\nu \sim \mathcal{O}(10^{-6})$ can reproduce the neutrino mass and mixing data [74]. As before, flavor mixings in the slepton sector can be induced radiatively by the off-diagonal entries in the neutrino Yukawa coupling, which are suppressed due to the smallness of Yukawa couplings. However, for simplicity we assume neutrino Yukawa couplings to be diagonal which alleviates the slepton flavor mixings completely. The soft-supersymmetry-breaking scalar potential is given by,

$$V_{\text{soft}} = V_{\text{MSSM}} + \left(T_\lambda H_u \cdot H_d S + \frac{1}{3} T_\kappa S^3 \right. \\ \left. + T_\nu H_u \cdot \tilde{L} \tilde{\nu}_R^c + T_r S \tilde{\nu}_R^c \tilde{\nu}_R^c + \text{h.c.} \right) + m_{\tilde{\nu}_R}^2 |\tilde{\nu}_R^c|^2 + m_S^2 |S|^2, \quad (3.8)$$

where V_{MSSM} denotes the soft-supersymmetry breaking terms in the MSSM and $T_\nu \equiv T_{\nu_\alpha} y_{\nu_\alpha}$ where α denotes the generation indices. We do not assign VEV to $\tilde{\nu}_R^c$, thus R-parity is unbroken at the minimum of the scalar potential. In particular, the neutral scalar fields can develop, in general, the following vacuum expectation values at the minimum of the scalar potential.

$$\langle H_d^0 \rangle = v_d/\sqrt{2}; \quad \langle H_u^0 \rangle = v_u/\sqrt{2}; \quad \langle S \rangle = v_s/\sqrt{2}.$$

⁴Note that a complex value for T_ν leads to a mixing among the CP-even and CP-odd Higgses in the mass eigen-basis.

We further assume that y_r and T_r are flavor-diagonal for simplicity and consider the lightest $\tilde{\nu}_R^c$ as the lightest R-parity odd particle; and forefore the DM candidate.

We begin by decomposing the sneutrino fields in terms of real and imaginary components.

$$\begin{aligned}\tilde{\nu}_L &= \frac{1}{\sqrt{2}}(\phi_L + i\sigma_L), \\ \tilde{\nu}_R^c &= \frac{1}{\sqrt{2}}(\phi_R + i\sigma_R).\end{aligned}\tag{3.9}$$

where, ϕ_L, ϕ_R are the CP -even and σ_L, σ_R are the CP -odd scalar fields. The presence of $\Delta L = 2$ terms (for e.g. $y_r \hat{S} \hat{\nu}_R^c \hat{\nu}_R^c$) in the superpotential, and the corresponding soft-breaking term ($T_r \tilde{S} \tilde{\nu}_R^c \tilde{\nu}_R^c + \text{h.c.}$) can induce splitting between different CP-eigenstates of $\tilde{\nu}_R^c$.

The mass matrix for CP-even eigenstates (ϕ_L, ϕ_R) or for CP-odd eigenstates (σ_L, σ_R) is given by,

$$m_{\nu^{R,I}}^2 = \begin{pmatrix} m_{11}^{R,I} & m_{12}^{R,I} \\ m_{21}^{R,I} & m_{22}^{R,I} \end{pmatrix},\tag{3.10}$$

where,

$$\begin{aligned}m_{11}^{R,I} &= \frac{1}{8} \left(4v_u^2 y_\nu^2 + 8m_{\tilde{l}}^2 + (g_1^2 + g_2^2) (-v_u^2 + v_d^2) \right), \\ m_{12}^{R,I} = m_{21}^{R,I} &= \frac{1}{4} \left(2\sqrt{2}v_u T_\nu \pm v_s (\mp 2v_d \lambda y_\nu + 4v_u y_r y_\nu) \right), \\ m_{22}^{R,I} &= \frac{1}{4} \left(4m_R^2 + 8y_r^2 v_s^2 + 2y_\nu^2 v_u^2 \pm 2 \left((2\kappa v_s^2 - \lambda v_d v_u) y_r + 4\sqrt{2}T_r v_s - 2\lambda y_r v_u v_d \right) \right).\end{aligned}\tag{3.11}$$

The mass matrices can be diagonalized by unitary matrices Z^I and Z^R ,

$$\begin{aligned}Z^I m_{\nu^I}^2 Z^{I,\dagger} &= m_{\nu^I}^{D,2}, \\ Z^R m_{\nu^R}^2 Z^{R,\dagger} &= m_{\nu^R}^{D,2},\end{aligned}\tag{3.12}$$

where $m_{\nu^I}^D$ and $m_{\nu^R}^D$ denote the diagonalized mass matrices respectively, and the corresponding mass eigenstates are denoted by σ_i and ϕ_i ($i \in \{1, 2\}$); g_1 and g_2 are the $SU(2)_L$ gauge couplings; $m_{\tilde{l}}^2$ is the soft-supersymmetry breaking mass term for slepton doublet. The other parameters are described in eqs. (3.6) and (3.8). Generically, ϕ_i and σ_i are non-degenerate, thanks to the $\Delta L = 2$ term present in the superpotential.

In general, lightest of the states σ_i or ϕ_i could be the lightest SUSY particle in different regions of the parameter space. Depending on the choice of the parameters, σ_i or ϕ_i can have dominant gauge and/or Yukawa interactions. Their mass difference, defined by $\Delta m = |m_{\phi_i} - m_{\sigma_i}|$ cannot be arbitrary, especially when σ_i and ϕ_i have dominant left-handed component, i.e., σ_i and ϕ_i are of $\tilde{\nu}_L$ -type. In this case, the one-loop contributions to the neutrino mass matrix can be quite large which essentially limits $\Delta m \simeq 100$ keV [74, 94]. Moreover, due to its doublet nature under $SU(2)_L$, stringent constraints would also appear from the sneutrino-nucleus scattering (via t -channel Z boson exchange processes)

On the other hand, aforementioned constraints can be evaded naturally, if we assume that ϕ_1 and σ_1 are dominantly right-handed. In fact these states are completely unconstrained, and their splitting can be traced back to $\Delta L = 2$ terms present in the mass matrix.

parameter	A	B	C	parameter	A	B	C
$\tan\beta$	2.9	9.0	10.0	μ_{eff}	322	-273.2	-269.3
κ	0.712	0.713	0.713	T_κ	-45.14	277.9	273.92
y_r^{33}	0.18	0.506	0.50	T_r^{33}	-36.10	-79.98	-80.11
λ	0.719	0.73	0.719	T_λ	418	-1077	-1077
$m_{b_{1,2}^-}$	3200	3200	3200	$m_{\tilde{Q}}$	2000	2000	2000
$m_{\tilde{l}}$	300	300	300	m_{H_1}	126	125.8	127
m_{H_2}	332	260.14	259.92	m_{H_3}	1893	1810	1903
m_{A_s}	269.7	456.7	452	m_{A_3}	1891	1807	1903
m_{H^\pm}	1887	1803	1897	$m_{\tilde{\nu}_1^R}$	135	304	305
$m_{\tilde{\chi}_1^\pm}$	197	201.6	196	$m_{\tilde{\nu}_1^I}$	135	130.6	130
$m_{\tilde{\chi}_1^0}$	177	179.6	179	$m_{t_{1,2}^-}$	3200	3200	3200
$\sigma(\text{DM DM} \rightarrow \gamma\gamma)$ ($10^{-27} \text{ cm}^3 \text{ s}^{-1}$)	2.0	2.0	1.3	$\Omega_{\phi_1, \sigma_1} h^2$	0.11	0.10	0.09

Table 1. Benchmark points for σ_1 and/or ϕ_1 DM (co-) annihilation via (A) CP-odd Higgs pole; (B) CP-even Higgs pole with single component DM; and (C) CP-even Higgs pole with degenerate σ_1, σ_2 DM. All masses are shown in GeV.

However, nearly degenerate or degenerate σ_1 and ϕ_1 may be achieved, provided all $\Delta L = 2$ in combination vanishes. The condition for degeneracy, thus, can be expressed as,

$$\left(\left(-v_d v_u \lambda + v_s^2 \kappa \right) y_r + \sqrt{2} v_s T_r \right) = 0. \quad (3.13)$$

Though, it seems a bit fine-tuned, we find that, potentially testable photon signals can be achieved. Based on the above facts, we consider the following possibilities for a 130/135 GeV $\tilde{\nu}_R$ type dark matter, as presented in table 1.

Before discussing our results, a couple of comments are in order. In all our benchmark points, we have used resonance enhancement through light charginos to achieve the right annihilation cross-sections to $\gamma\gamma$ final state. This is quite generic and probably the simplest possibility in the context of SUSY scenarios to explain the rather large $\langle\sigma v\rangle_{\gamma\gamma}$ to fit the FERMI data. In the context of neutralino dark matter, the effect of resonance has already been well studied in the context of MSSM and NMSSM. Clearly, the resonance condition leads to fine-tuning on the parameter space which diminishes the naturalness of the model. In the present case $|M_{H_s} - 2m_{\tilde{\nu}_R}| \lesssim 1.0 \text{ GeV}$ is an appropriate requirement. However, the right thermal relic density can be obtained when $2m_{\tilde{\nu}_R} - M_{H_s} \gtrsim 0$, around the resonance. For $2m_{\tilde{\nu}_R} - M_{H_s} \lesssim 0$, the thermal relic abundance, typically, becomes too low and additional (possibly non-thermal) production of dark matter is required. Moreover, the rate of the photon signal can be enhanced with a less fine-tuned M_{H_s} if a larger $H_s - \gamma - \gamma$ amplitude occurs. This is possible through the participation of (a) light charginos (and/or charged Higgses) which are already a part of this model, and (b) charged vector-like $\text{SU}(2)_L$ singlet

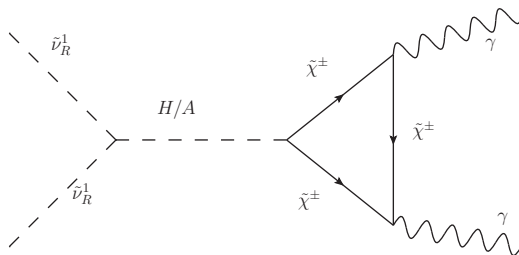


Figure 1. The dominant annihilation diagram for $\tilde{\nu}_R$ -like DM into two photons via a singlet-like CP-even/CP-odd Higgs H/A in the NMSSM. Similar diagrams with (s)quarks and (s)leptons running in the loop contribute negligibly.

fermions. Furthermore, the advantage of considering right handed sneutrino as dark matter is that it can largely evade the very stringent direct detection constraints which otherwise forbid a large part of the parameter space.

3.2.1 ϕ_1/σ_1 dark matter

In the first scenario, we illustrate how CP eigenstates ϕ_1 or σ_1 can annihilate through singlet-like CP-even Higgs (H_2) resonance to $\gamma\gamma$ (see figure 1). The singlet nature of H_2 helps to accommodate constraints from the continuum γ . In addition, the narrow width of a singlet-like H_2 also reduces the contribution of the resonance mediated channels to the relic density.

The couplings $C_{r,o}$ in eq. (2.3), between the singlet-like CP-even Higgs and ϕ_1/σ_1 takes the following form,

$$\begin{aligned} C_r &\simeq \sqrt{2}T_r Z_{23}^H Z_{12}^{R2} + v_s (2\kappa y_r + y_r^2) Z_{23}^H Z_{12}^{R2} + \dots \\ C_o &\simeq -\sqrt{2}T_r Z_{23}^H Z_{12}^{I2} - v_s (2\kappa y_r - y_r^2) Z_{23}^H Z_{12}^{I2} + \dots \end{aligned} \quad (3.14)$$

The term proportional to T_r comes from the soft-supersymmetry breaking sector, while the other terms come from the F-term contributions to the scalar potential. Z^H represents the mixing matrix of the CP-even Higgs bosons. Assuming that the second lightest CP-even Higgs (singlet-like) boson contributes dominantly, Z_{23}^H is the relevant entry in eq. (3.14) while the ellipsis indicate the sub-leading contributions originating from small doublet components. These couplings play crucial roles in determining both $\langle\sigma v\rangle_{\gamma\gamma}$ and the thermal relic abundance.

The desired signal $\langle\sigma v\rangle_{\gamma\gamma}$ can be easily enhanced with larger $C_{o/r}$ and/or λ . Larger values of λ can enhance the effective coupling of $H_2 - \gamma - \gamma$ via $\lambda H_2(S)\tilde{H}_u^+\tilde{H}_d^-$ loops in eq. (3.6). Since the contribution from the charginos (χ^\pm) running in the loop dominates, light higgsino-like χ^\pm are desired to enhance the signal. In figure 2, we present $\langle\sigma v\rangle_{\gamma\gamma}$ with representative values of the input parameters around the Higgs threshold. Interestingly, we can easily obtain the $\langle\sigma v\rangle_{\gamma\gamma}$ with the pole mass below or above the threshold, i.e. ($2m_{\sigma_1/\phi_1}$). However, the correct thermal relic density can be obtained only when the pole is below the threshold, as shown in the left panel of figure 3. To understand it better, we also depict the parameter x_f (i.e. m/T_f , as already discussed in section 2), which characterises the freeze-out, against M_H in the figure 4. As can be seen from figure 4, x_f is larger for M_H above the threshold (260 GeV), implying late freeze-out compared to the scenario when M_H is below the threshold. A lower relic density in this region corresponds to the fact that for $\delta < 0$ the pole would be physical when the dark matter particles have high kinetic energy in the early

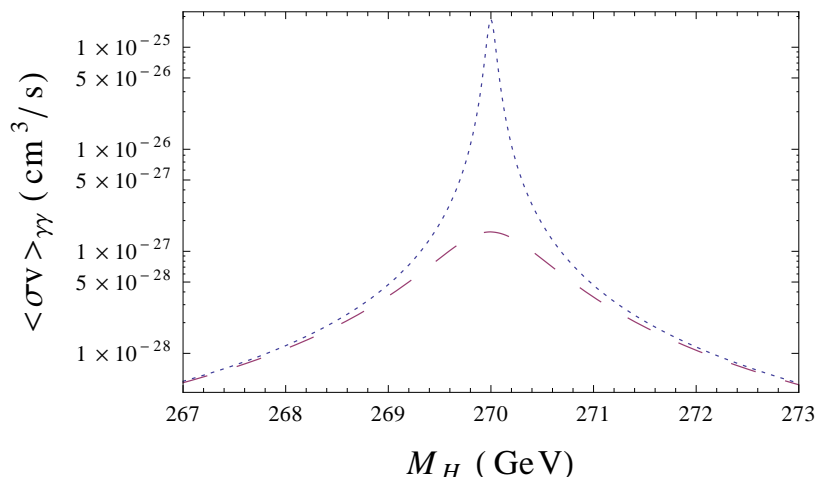


Figure 2. The enhancement of the $\langle\sigma v\rangle_{\gamma\gamma}$ in the vicinity of the resonance, above and below the pole (270 GeV) is shown here. The blue (dotted) curve represents a total width of 0.1 GeV below the threshold while the red (dashed) curve represents a width of 1.1 GeV in the same region.

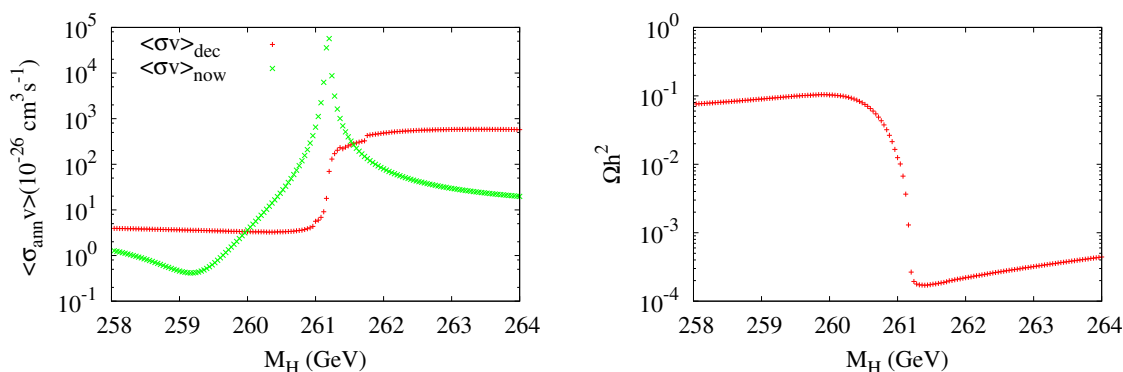


Figure 3. Relic density of σ_1 DM, with a mass of 130.6 GeV, has been plotted against the singlet-like CP-even Higgs pole mass. In the left panel the thermally averaged cross-sections at freeze-out temperature (T_f) and at late time (the speed of DM $v \sim 0.001$ or $T = T_0 \sim 10^{-4}$ GeV) have been shown in red and green respectively. In the right panel the CP-even Higgs mass is varied to demonstrate the relic abundance below and above the threshold (261.2 GeV). All other relevant parameters have been mentioned in column (B) of table 1.

Universe. Thus, resonant annihilation will lead to a large thermally averaged annihilation cross-section around the time of freeze-out. This, in turn, leads to a lower relic density. A more detailed discussion on this point has already been included in section 2.

As noted in eq. (3.14) and eq. (3.11), both the couplings $C_{r,o}$, as well as the mass of σ_1 , depend on T_r and y_r , while the other free parameters involved in these equations also affect, among others, the Higgs sector. Therefore, in figure 5, we present the allowed parameter space in the (T_r, y_r) plane; assuming the following input parameters (at the SUSY scale):

$$\lambda = 0.73, \quad \kappa = 0.713, \quad T_\lambda = -1077, \quad T_\kappa = 277.92, \quad \tan\beta = 10.$$

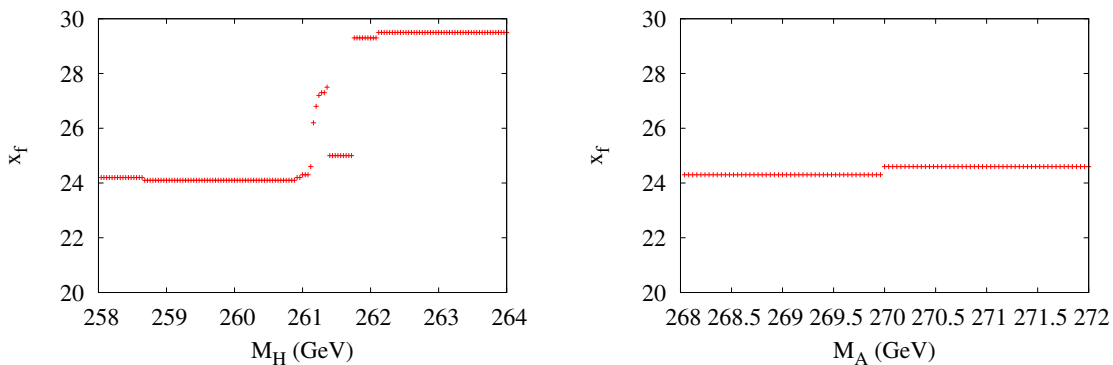


Figure 4. $x_f = \frac{m_{\sigma_1}}{T_f}$, where σ_1 is dark matter, around the singlet-like (a) CP-even Higgs pole and (b) CP-odd Higgs pole have been plotted. Note that, for our benchmark points, m_{ϕ_1/σ_1} is 130 GeV (135 GeV) for the CP-even (CP-odd) Higgs resonance respectively. This figure depicts the late freeze-out of the DM when the mass of the DM is less than half of the CP-even/CP-odd Higgs mass, i.e. when the physical pole is encountered.

Our choice for these parameters are consistent with the LHC data on the SM-like CP-even Higgs while providing us with another singlet-like CP-even Higgs with a mass of 260 GeV. All other parameters are set to alleviate LHC constraints as mentioned in section 3. We also set soft breaking parameter of the right handed sneutrino so to have σ_1 as LSP with mass 130.5 GeV. With the given parameters, we obtain $m_{H_{SM}} = 125.7$ GeV while for the singlet like Higgs we get $m_{H_2} = 260.1$ GeV. Assuming, for simplicity, that the third generation right handed sneutrino as the LSP, we only varied T_r^{33} and y_r^{33} to delineate the WMAP satisfied region in the vicinity of H_2 resonance. In this region, due to the singlet nature of H_2 and the smallness of the coupling among $\sigma_1 - H_2 - \sigma_1$, the annihilation channels mediated by the lightest CP-even Higgs boson contributes significantly in satisfying the relic density. These points are also allowed by the recent bounds from LUX [57]. Interestingly, the whole parameter space can provide with adequate cross-section for $\langle\sigma v\rangle_{\gamma\gamma}$.

For the benchmark point presented in column (B) of table 1, we assume σ_1 to be the DM.⁵ The representative values, as shown in column (B) of table 1 satisfy the desired $\langle\sigma v\rangle_{\gamma\gamma}$ and other mentioned constraints including WMAP. In the calculation of $\langle\sigma v\rangle_{\gamma\gamma}$, we have $\text{Br}(H_2 \rightarrow \gamma\gamma) = 1.5 \times 10^{-4}$, $\Gamma_H = 0.02$ GeV and $\delta = 0.007$ (see eq. (2.3)). We also consider another simple scenario, where σ_1 is not the sole component of the dark matter density. For example, if the second lightest CP-odd sneutrino eigenstates, σ_2 is degenerate with σ_1 , then it will be present during the time of decoupling to contribute to the relic abundance. An example is depicted in column (C) of table 1 which possesses the desired values of the thermal relic density and $\langle\sigma v\rangle_{\gamma\gamma}$.

3.2.2 Degenerate ϕ_1 - σ_1 dark matter

Both of these components can be present today, if their masses are (near) degenerate.⁶ In this case, this degenerate DM annihilates through singlet-like CP odd Higgs (A_s) resonance

⁵Note that by simply reversing the signs of y_r and T_r , one can have CP-even ϕ_1 as the LSP while the mass spectra remains unchanged. Consequently, one can explain the observed γ signal with CP-even ϕ_1 DM.

⁶Mass splitting Δ_m between ϕ_1, σ_1 should be much less than $\mathcal{O}(100$ keV), so that the heavier state is sufficiently long-lived.

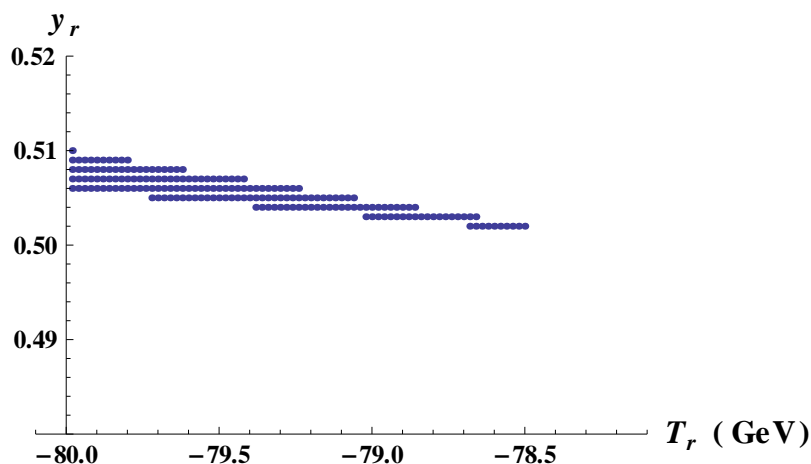


Figure 5. WMAP allowed parameter space for σ_1 DM, with a mass of 130 GeV, has been shown in the T_r, y_r plane. All these points satisfy direct detection limits from LUX while having adequate cross-section to account for the photon signal.

to $\gamma\gamma$, as illustrated in figure 1. Similar to the previous case, a singlet-like CP-odd Higgs, with dominant branching ratio to di-photon final state, helps in satisfying the continuum constraints; while enhancing DM annihilation cross-section to di-photon final state in the vicinity of the narrow resonance.

To estimate $\langle\sigma v\rangle_{\gamma\gamma}$, as mentioned, we use eq. (2.3). The coupling C of the singlet-like CP-odd Higgs (A_s) with $\sigma_1 - \phi_1$, in the gauge eigen-basis, is given by,

$$C = -2\kappa v_s y_r Z_{s3}^A Z_{12}^I Z_{12}^R - \sqrt{2} Z_{s3}^A T_r Z_{12}^I Z_{12}^R; \quad (3.15)$$

where, Z^A denotes the mixing matrices of the CP-odd Higgs and all other symbols are as defined before.

As in the previous case, $\langle\sigma v\rangle_{\gamma\gamma}$ can easily be enhanced by increasing C (thus y_r and/or λ), but that could lead to small relic abundance. A light higgsino-like χ^\pm is desired to enhance the same. Again, we consider $m_{A_s} < 2m_{\phi_1 - \sigma_1}$, i.e., part of the parameter space where the pole of the propagator is below the threshold, to obtain the right thermal relic abundance. In particular, here we require extremely singlet like pseudo-scalar Higgs so that $\text{Br}(A_s \rightarrow \gamma\gamma)$ (see eq. (2.3)) can be very large to account for the desired $\langle\sigma v\rangle_{\gamma\gamma}$. Also, the coupling C should be small so that the correct relic abundance can be obtained through the processes mediated by the other Higgs states. This in turn prefers small values of y_r if one does not want to have unnatural cancellation among different parameters in eq. (3.15). However, here for $\delta > 0$ (see section 2), below the threshold, in our region of interest, we find A_s dominantly decays to a pair of ν_R which can substantially enhance the decay width of A_s . It also affects the DM density as DM can also annihilate in to a pair of ν_R via A_s resonance leading to a small relic density. To circumvent this problem, we add an additional Majorana mass term ($m_N \nu_R \nu_R$) to the Lagrangian which enhance the masses for sterile neutrinos to kinematically forbids this decay channel. Thus the pole can appear very close to the threshold and $\langle\sigma v\rangle_{\gamma\gamma}$ can be extremely large in this region (as the branching fraction $A_s \rightarrow \gamma\gamma$ can be as large as $\sim 70\%$).

To demonstrate our results, we present in the left panel of figure 6, the thermally averaged cross-section, when the pole falls above the threshold (270 GeV), is a little larger

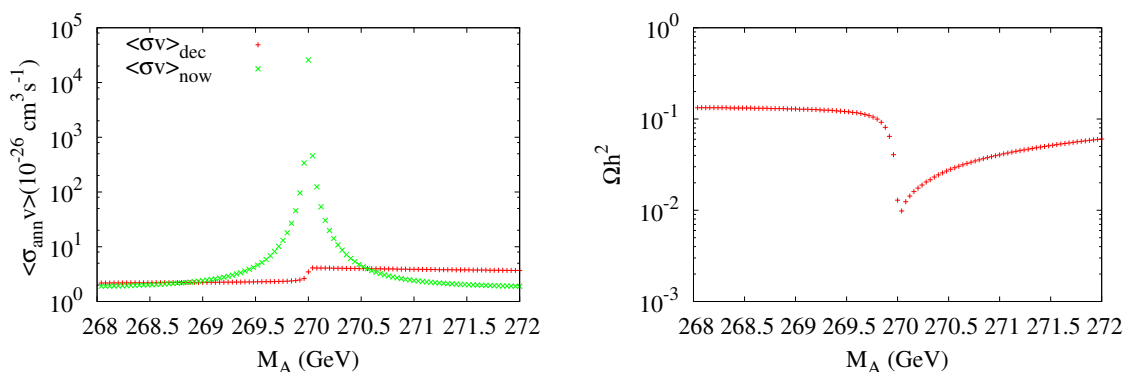


Figure 6. Relic density of mixed ϕ_1 , σ_1 type DM with a mass of 135 GeV, has been plotted against the singlet-like CP-odd Higgs pole mass. In the left panel the thermally averaged cross-sections at freeze-out temperature (T_f) and at late time (the speed of DM $v \sim 0.001$ or $T = T_0 \sim 10^{-4}$ GeV) have been shown in red and green respectively. In the right panel the CP-odd Higgs mass is varied to demonstrate the relic abundance below and above the threshold (270 GeV).

than the same when the pole falls below the threshold. Also, as the right panel of figure 6 shows, in the former case, freeze-out happens a little later. Consequently, the thermal relic abundance decreases in the former case. Note that, due to the much smaller width of A_s compared to that of H_2 in the previous case, the effect of the resonance on the relic density is quite small.

A benchmark point in column (A) of table 1 has been presented to summarize the results. The relic density can be obtained mainly via the annihilation channels mediated via the off-shell CP-even Higgs bosons. In the calculation of $\langle\sigma v\rangle_{\gamma\gamma}$, we have $\text{Br}(A_s \rightarrow \gamma\gamma) \simeq 5 \times 10^{-4}$, $\Gamma_{A_s} = 0.003$ GeV and $\delta = 0.002$. All phenomenological constraints, from both direct and indirect detection data, can easily be satisfied for the benchmark point (A) shown in table 1, thanks to the singlet nature of A_s .

3.2.3 Constraints from direct detection

An interesting issue for the models, which give the desired $\langle\sigma v\rangle_{\gamma\gamma}$, is to address constraints coming from the spin-independent direct detection, particularly in the light of XENON-100 and LUX data. In the NMSSM, the parameter space for a 130/135 GeV neutralino DM, achieving the desired $\langle\sigma v\rangle_{\gamma\gamma}$, is constrained by the present bound $\sigma(p)_{SI} \lesssim 1.2 \times 10^{-8}$ pb and $\sigma_{SI} \lesssim 1.5 \times 10^{-9}$ pb for $M_{DM} \sim 130/135$ GeV from XENON-100 [56] and LUX [57] respectively. An important issue concerns the quark coefficient in the nucleon which may lead to large theoretical uncertainty in the calculation. In this work, we always keep the default values that are used in micrOMEGAs-3.

Being a real scalar, ϕ_1 (σ_1) interacts with nucleons via Higgs exchange processes. As the Yukawa coupling is very small ($\sim 10^{-7}$), the coupling $\phi_1/\sigma_1 - H - \phi_1/\sigma_1$ is principally determined by $T_r S \tilde{\nu}_R^c \tilde{\nu}_R^c$ and $\kappa v_s S^* \tilde{\nu}_R^c \tilde{\nu}_R^c$, $\lambda y_r v_{u,d} H_{d,u}^* \tilde{\nu}_R^c \tilde{\nu}_R^c$ terms, arising from the soft-breaking sector and the F-term contributions respectively. Singlet-like Higgs does not couple to the quarks or gluons at tree-level, while the coupling of the doublet-like Higgs with $\tilde{\nu}_R^c \tilde{\nu}_R^c$ is quite small. Also, since both ϕ_1 and σ_1 are dominantly right-chiral, Z boson exchange does not lead to large $\sigma(p)_{SI}$ even when these are degenerate. The only term, which gives rise to dominant contribution to $\sigma(p)_{SI}$ originates from the F-term contribution ($\lambda \frac{y_r}{2} \tilde{\nu}_R \tilde{\nu}_R H_u \cdot H_d + \text{h.c.}$).

While both λ and y_r appears in $\langle\sigma v\rangle_{\gamma\gamma}$, note that it is possible to achieve large $\langle\sigma v\rangle_{\gamma\gamma}$ with small y_r by increasing the soft-term T_r appropriately. In summary, the scenarios proposed here are not significantly constrained by the XENON-100, these are moderately constrained by the LUX data.

4 Summary and Conclusions

We have explored the possibility that the annihilation of 130/135 GeV right-chiral sneutrino DM into two photons can produce the observed line-like feature in the Fermi-LAT data. In this context, we examine the candidature of right-sneutrino dark matter — a scenario that can have somewhat unusual phenomenological implications. It is, however, seen that the augmentation of the MSSM just with right-chiral neutrino superfields is inadequate. The difficulty arises from severe constraints on various annihilation channels of the dark matter, most notably into ZH and $b\bar{b}$, derived from the continuum flux of photons. However, in the extension of the next-to-minimal model (NMSSM), annihilating right-chiral sneutrino DM, can produce the observed line feature. Due to the extra singlet field present in this model, a singlet-like CP-odd or CP-even Higgs boson resonance produces adequate annihilation cross-section to fit the observation. We find that in case of a CP-odd Higgs resonance, one needs the lightest CP-even and the lightest CP-odd right-chiral sneutrino states to be (almost) degenerate. In the latter case however, this is not a requirement. We present a few benchmark points to substantiate our claims and highlight the spectrum which is consistent with the data. While our benchmark points also satisfy the present direct detection bounds, improved bounds in near future may be able to explore the viability of our scenario. In addition, we show that when the pole in the resonance is a little below twice the mass of the DM, the thermal production of right-chiral sneutrino dark matter can be sufficient to also account for the DM abundance, as required by the CMBR data, especially in the case of degeneracy in the sneutrino sector.

Acknowledgments

AC and DD would like to thank Florian Staub for useful discussions about the code SARAH. The work of AC, BM and SKR was partially supported by funding available from the Department of Atomic Energy, Government of India, for the Regional Centre for Accelerator-based Particle Physics (RECAPP), Harish-Chandra Research Institute (HRI). DD acknowledges support received from the DFG, project no. PO-1337/3-1 at the Universität Würzburg. DD thanks RECAPP, Allahabad, for hospitality during the initial part of the project.

References

- [1] LAT collaboration, W.B. Atwood et al., *The Large Area Telescope on the Fermi Gamma-ray Space Telescope Mission*, *Astrophys. J.* **697** (2009) 1071 [[arXiv:0902.1089](#)] [[INSPIRE](#)].
- [2] T. Bringmann, X. Huang, A. Ibarra, S. Vogl and C. Weniger, *Fermi LAT Search for Internal Bremsstrahlung Signatures from Dark Matter Annihilation*, *JCAP* **07** (2012) 054 [[arXiv:1203.1312](#)] [[INSPIRE](#)].
- [3] C. Weniger, *A Tentative Gamma-Ray Line from Dark Matter Annihilation at the Fermi Large Area Telescope*, *JCAP* **08** (2012) 007 [[arXiv:1204.2797](#)] [[INSPIRE](#)].

- [4] E. Tempel, A. Hektor and M. Raidal, *Fermi 130 GeV gamma-ray excess and dark matter annihilation in sub-haloes and in the Galactic centre*, *JCAP* **09** (2012) 032 [Addendum *ibid.* **1211** (2012) A01] [[arXiv:1205.1045](#)] [[INSPIRE](#)].
- [5] M. Su and D.P. Finkbeiner, *Strong Evidence for Gamma-ray Lines from the Inner Galaxy*, [arXiv:1206.1616](#).
- [6] A. Hektor, M. Raidal and E. Tempel, *An evidence for indirect detection of dark matter from galaxy clusters in Fermi-LAT data*, *Astrophys. J.* **762** (2013) L22 [[arXiv:1207.4466](#)] [[INSPIRE](#)].
- [7] M. Su and D.P. Finkbeiner, *Double Gamma-ray Lines from Unassociated Fermi-LAT Sources*, [arXiv:1207.7060](#).
- [8] D. Hooper and T. Linden, *Are Lines From Unassociated Gamma-Ray Sources Evidence For Dark Matter Annihilation?*, *Phys. Rev. D* **86** (2012) 083532 [[arXiv:1208.0828](#)] [[INSPIRE](#)].
- [9] N. Mirabal, *The Dark Knight Falters*, *Mon. Not. Roy. Astron. Soc.* **429** (2013) L109 [[arXiv:1208.1693](#)] [[INSPIRE](#)].
- [10] A. Hektor, M. Raidal and E. Tempel, *Double gamma-ray lines from unassociated Fermi-LAT sources revisited*, [arXiv:1208.1996](#).
- [11] H.-S. Zechlin and D. Horns, *Unidentified sources in the Fermi-LAT second source catalog: the case for DM subhalos*, *JCAP* **11** (2012) 050 [[arXiv:1210.3852](#)] [[INSPIRE](#)].
- [12] A. Rajaraman, T.M.P. Tait and D. Whiteson, *Two Lines or Not Two Lines? That is the Question of Gamma Ray Spectra*, *JCAP* **09** (2012) 003 [[arXiv:1205.4723](#)] [[INSPIRE](#)].
- [13] T. Bringmann and C. Weniger, *Gamma Ray Signals from Dark Matter: Concepts, Status and Prospects*, *Phys. Dark Univ.* **1** (2012) 194 [[arXiv:1208.5481](#)].
- [14] FERMI-LAT collaboration, A. Albert et al., *Search for Gamma-ray Spectral Lines with the Fermi Large Area Telescope and Dark Matter Implications*, *Phys. Rev. D* **88** (2013) 082002 [[arXiv:1305.5597](#)].
- [15] A. Albert, *Search for Gamma-ray Spectral Lines in the Milky Way Diffuse with the Fermi Large Area Telescope*, talk given at *Fourth International Fermi Symposium*, Monterey, California, 28 October–2 November 2012, <http://fermi.gsfc.nasa.gov/science/mtgs/symposia/2012/program/fri/AAlbert.pdf>.
- [16] S. Profumo and T. Linden, *Gamma-ray Lines in the Fermi Data: is it a Bubble?*, *JCAP* **07** (2012) 011 [[arXiv:1204.6047](#)] [[INSPIRE](#)].
- [17] A. Boyarsky, D. Malyshev and O. Ruchayskiy, *Spectral and spatial variations of the diffuse γ -ray background in the vicinity of the Galactic plane and possible nature of the feature at 130 GeV*, *Phys. Dark Univ.* **2** (2013) 90 [[arXiv:1205.4700](#)].
- [18] J.M. Cline, *130 GeV dark matter and the Fermi gamma-ray line*, *Phys. Rev. D* **86** (2012) 015016 [[arXiv:1205.2688](#)] [[INSPIRE](#)].
- [19] H.M. Lee, M. Park and W.-I. Park, *Fermi Gamma Ray Line at 130 GeV from Axion-Mediated Dark Matter*, *Phys. Rev. D* **86** (2012) 103502 [[arXiv:1205.4675](#)] [[INSPIRE](#)].
- [20] E. Dudas, Y. Mambrini, S. Pokorski and A. Romagnoni, *Extra $U(1)$ as natural source of a monochromatic gamma ray line*, *JHEP* **10** (2012) 123 [[arXiv:1205.1520](#)] [[INSPIRE](#)].
- [21] K.-Y. Choi and O. Seto, *A Dirac right-handed sneutrino dark matter and its signature in the gamma-ray lines*, *Phys. Rev. D* **86** (2012) 043515 [Erratum *ibid.* **D 86** (2012) 089904] [[arXiv:1205.3276](#)] [[INSPIRE](#)].
- [22] B. Kyae and J.-C. Park, *130 GeV Fermi gamma-ray line from dark matter decay*, *Phys. Lett. B* **718** (2013) 1425 [[arXiv:1205.4151](#)] [[INSPIRE](#)].

- [23] B.S. Acharya, G. Kane, P. Kumar, R. Lu and B. Zheng, *Mixed Wino-Axion Dark Matter in String/M Theory and the 130 GeV Gamma-line “Signal”*, [arXiv:1205.5789](#).
- [24] M.R. Buckley and D. Hooper, *Implications of a 130 GeV Gamma-Ray Line for Dark Matter*, *Phys. Rev. D* **86** (2012) 043524 [[arXiv:1205.6811](#)] [[INSPIRE](#)].
- [25] X. Chu, T. Hambye, T. Scarna and M.H.G. Tytgat, *What if Dark Matter Gamma-Ray Lines come with Gluon Lines?*, *Phys. Rev. D* **86** (2012) 083521 [[arXiv:1206.2279](#)] [[INSPIRE](#)].
- [26] N. Weiner and I. Yavin, *How Dark Are Majorana WIMPs? Signals from MiDM and Rayleigh Dark Matter*, *Phys. Rev. D* **86** (2012) 075021 [[arXiv:1206.2910](#)] [[INSPIRE](#)].
- [27] J.H. Heo and C.S. Kim, *Dipole-interacting Fermionic Dark Matter in positron, antiproton and gamma-ray channels*, *Phys. Rev. D* **87** (2013) 013007 [[arXiv:1207.1341](#)] [[INSPIRE](#)].
- [28] M.T. Frandsen, U. Haisch, F. Kahlhoefer, P. Mertsch and K. Schmidt-Hoberg, *Loop-induced dark matter direct detection signals from gamma-ray lines*, *JCAP* **10** (2012) 033 [[arXiv:1207.3971](#)] [[INSPIRE](#)].
- [29] J.-C. Park and S.C. Park, *Radiatively decaying scalar dark matter through $U(1)$ mixings and the Fermi 130 GeV gamma-ray line*, *Phys. Lett. B* **718** (2013) 1401 [[arXiv:1207.4981](#)] [[INSPIRE](#)].
- [30] S. Tulin, H.-B. Yu and K.M. Zurek, *Three Exceptions for Thermal Dark Matter with Enhanced Annihilation to $\gamma\gamma$* , *Phys. Rev. D* **87** (2013) 036011 [[arXiv:1208.0009](#)].
- [31] J.M. Cline, A.R. Frey and G.D. Moore, *Composite magnetic dark matter and the 130 GeV line*, *Phys. Rev. D* **86** (2012) 115013 [[arXiv:1208.2685](#)] [[INSPIRE](#)].
- [32] L. Bergstrom, *The 130 GeV Fingerprint of Right-Handed Neutrino Dark Matter*, *Phys. Rev. D* **86** (2012) 103514 [[arXiv:1208.6082](#)] [[INSPIRE](#)].
- [33] N. Weiner and I. Yavin, *UV Completions of Magnetic Inelastic Dark Matter and RayDM for the Fermi Line(s)*, *Phys. Rev. D* **87** (2013) 023523 [[arXiv:1209.1093](#)] [[INSPIRE](#)].
- [34] J. Fan and M. Reece, *A Simple Recipe for the 111 and 128 GeV Lines*, *Phys. Rev. D* **88** (2013) 035014 [[arXiv:1209.1097](#)].
- [35] H.M. Lee, M. Park and W.-I. Park, *Axion-mediated dark matter and Higgs diphoton signal*, *JHEP* **12** (2012) 037 [[arXiv:1209.1955](#)] [[INSPIRE](#)].
- [36] L. Wang and X.-F. Han, *130 GeV gamma-ray line and enhancement of $h \rightarrow \gamma\gamma$ in the Higgs triplet model plus a scalar dark matter*, *Phys. Rev. D* **87** (2013) 015015 [[arXiv:1209.0376](#)] [[INSPIRE](#)].
- [37] F. D’Eramo, M. McCullough and J. Thaler, *Multiple Gamma Lines from Semi-Annihilation*, *JCAP* **04** (2013) 030 [[arXiv:1210.7817](#)].
- [38] N. Bernal, C. Boehm, S. Palomares-Ruiz, J. Silk and T. Toma, *Observing Higgs boson production through its decay into γ -rays: A messenger for Dark Matter candidates*, *Phys. Lett. B* **723** (2013) 100 [[arXiv:1211.2639](#)].
- [39] Y. Farzan and A.R. Akbarieh, *Natural explanation for 130 GeV photon line within vector boson dark matter model*, *Phys. Lett. B* **724** (2013) 84 [[arXiv:1211.4685](#)].
- [40] Y. Bai and J. Shelton, *Gamma Lines without a Continuum: Thermal Models for the Fermi-LAT 130 GeV Gamma Line*, *JHEP* **12** (2012) 056 [[arXiv:1208.4100](#)] [[INSPIRE](#)].
- [41] D. Das, U. Ellwanger and P. Mitropoulos, *A 130 GeV photon line from dark matter annihilation in the NMSSM*, *JCAP* **08** (2012) 003 [[arXiv:1206.2639](#)] [[INSPIRE](#)].
- [42] Z. Kang, J. Li, T. Li and Y. Liu, *Brightening the (130 GeV) Gamma-Ray Line*, [arXiv:1206.2863](#).
- [43] W. Buchmüller and M. Garny, *Decaying vs Annihilating Dark Matter in Light of a Tentative Gamma-Ray Line*, *JCAP* **08** (2012) 035 [[arXiv:1206.7056](#)] [[INSPIRE](#)].

- [44] I. Cholis, M. Tavakoli and P. Ullio, *Searching for the continuum spectrum photons correlated to the 130 GeV gamma-ray line*, *Phys. Rev. D* **86** (2012) 083525 [[arXiv:1207.1468](#)] [[INSPIRE](#)].
- [45] T. Cohen, M. Lisanti, T.R. Slatyer and J.G. Wacker, *Illuminating the 130 GeV Gamma Line with Continuum Photons*, *JHEP* **10** (2012) 134 [[arXiv:1207.0800](#)] [[INSPIRE](#)].
- [46] X. Huang, Q. Yuan, P.-F. Yin, X.-J. Bi and X. Chen, *Constraints on the dark matter annihilation scenario of Fermi 130 GeV γ -ray line emission by continuous gamma-rays, Milky Way halo, galaxy clusters and dwarf galaxies observations*, *JCAP* **11** (2012) 048 [Erratum *ibid.* **1305** (2013) E02] [[arXiv:1208.0267](#)] [[INSPIRE](#)].
- [47] G. Chalons, M.J. Dolan and C. McCabe, *Neutralino dark matter and the Fermi gamma-ray lines*, *JCAP* **02** (2013) 016 [[arXiv:1211.5154](#)].
- [48] T. Basak and S. Mohanty, *130 GeV gamma ray line and enhanced Higgs di-photon rate from Triplet-Singlet extended MSSM*, *JHEP* **08** (2013) 020 [[arXiv:1304.6856](#)] [[INSPIRE](#)].
- [49] G. Tomar, S. Mohanty and S. Rao, *130 GeV Gamma Ray Signal in NMSSM by Internal Bremsstrahlung*, [arXiv:1306.3646](#).
- [50] T. Basak and T. Mondal, *Constraining Minimal $U(1)_{B-L}$ model from Dark Matter Observations*, *Phys. Rev. D* **89** (2014) 063527 [[arXiv:1308.0023](#)].
- [51] T. Toma, *Internal Bremsstrahlung Signature of Real Scalar Dark Matter and Consistency with Thermal Relic Density*, *Phys. Rev. Lett.* **111** (2013) 091301 [[arXiv:1307.6181](#)] [[INSPIRE](#)].
- [52] F. Giacchino, L. Lopez-Honorez and M.H.G. Tytgat, *Scalar Dark Matter Models with Significant Internal Bremsstrahlung*, *JCAP* **10** (2013) 025 [[arXiv:1307.6480](#)] [[INSPIRE](#)].
- [53] F. Boudjema, A. Semenov and D. Temes, *Self-annihilation of the neutralino dark matter into two photons or a Z and a photon in the MSSM*, *Phys. Rev. D* **72** (2005) 055024 [[hep-ph/0507127](#)] [[INSPIRE](#)].
- [54] F. Ferrer, L.M. Krauss and S. Profumo, *Indirect detection of light neutralino dark matter in the NMSSM*, *Phys. Rev. D* **74** (2006) 115007 [[hep-ph/0609257](#)] [[INSPIRE](#)].
- [55] G. Chalons and A. Semenov, *Loop-induced photon spectral lines from neutralino annihilation in the NMSSM*, *JHEP* **12** (2011) 055 [[arXiv:1110.2064](#)] [[INSPIRE](#)].
- [56] XENON100 collaboration, E. Aprile et al., *Dark Matter Results from 225 Live Days of XENON100 Data*, *Phys. Rev. Lett.* **109** (2012) 181301 [[arXiv:1207.5988](#)] [[INSPIRE](#)].
- [57] LUX collaboration, D.S. Akerib et al., *First results from the LUX dark matter experiment at the Sanford Underground Research Facility*, *Phys. Rev. Lett.* **112** (2014) 091303 [[arXiv:1310.8214](#)].
- [58] B. Shakya, *A 130 GeV Gamma Ray Signal from Supersymmetry*, *Phys. Dark Univ.* **2** (2013) 83 [[arXiv:1209.2427](#)].
- [59] WMAP collaboration, E. Komatsu et al., *Seven-Year Wilkinson Microwave Anisotropy Probe (WMAP) Observations: Cosmological Interpretation*, *Astrophys. J. Suppl.* **192** (2011) 18 [[arXiv:1001.4538](#)] [[INSPIRE](#)].
- [60] T. Asaka, K. Ishiwata and T. Moroi, *Right-handed sneutrino as cold dark matter*, *Phys. Rev. D* **73** (2006) 051301 [[hep-ph/0512118](#)] [[INSPIRE](#)].
- [61] T. Asaka, K. Ishiwata and T. Moroi, *Right-handed sneutrino as cold dark matter of the universe*, *Phys. Rev. D* **75** (2007) 065001 [[hep-ph/0612211](#)] [[INSPIRE](#)].
- [62] S. Gopalakrishna, A. de Gouvêa and W. Porod, *Right-handed sneutrinos as nonthermal dark matter*, *JCAP* **05** (2006) 005 [[hep-ph/0602027](#)] [[INSPIRE](#)].
- [63] R. Allahverdi, B. Dutta and A. Mazumdar, *Unifying inflation and dark matter with neutrino masses*, *Phys. Rev. Lett.* **99** (2007) 261301 [[arXiv:0708.3983](#)] [[INSPIRE](#)].

- [64] D. Choudhury, S.K. Gupta and B. Mukhopadhyaya, *Right sneutrinos in a supergravity model and the signals of a stable stop at the Large Hadron Collider*, *Phys. Rev. D* **78** (2008) 015023 [[arXiv:0804.3560](#)] [[INSPIRE](#)].
- [65] S.K. Gupta, B. Mukhopadhyaya and S.K. Rai, *Right-chiral sneutrinos and long-lived staus: Event characteristics at the large hadron collider*, *Phys. Rev. D* **75** (2007) 075007 [[hep-ph/0701063](#)] [[INSPIRE](#)].
- [66] S. Biswas and B. Mukhopadhyaya, *Chargino reconstruction in supersymmetry with long-lived staus*, *Phys. Rev. D* **81** (2010) 015003 [[arXiv:0910.3446](#)] [[INSPIRE](#)].
- [67] S. Biswas and B. Mukhopadhyaya, *Neutralino reconstruction in supersymmetry with long-lived staus*, *Phys. Rev. D* **79** (2009) 115009 [[arXiv:0902.4349](#)] [[INSPIRE](#)].
- [68] S. Banerjee, P.S.B. Dev, S. Mondal, B. Mukhopadhyaya and S. Roy, *Invisible Higgs Decay in a Supersymmetric Inverse Seesaw Model with Light Sneutrino Dark Matter*, *JHEP* **10** (2013) 221 [[arXiv:1306.2143](#)] [[INSPIRE](#)].
- [69] P.S. Bhupal Dev, S. Mondal, B. Mukhopadhyaya and S. Roy, *Phenomenology of Light Sneutrino Dark Matter in cMSSM/mSUGRA with Inverse Seesaw*, *JHEP* **09** (2012) 110 [[arXiv:1207.6542](#)] [[INSPIRE](#)].
- [70] J. Guo, Z. Kang, T. Li and Y. Liu, *Higgs boson mass and complex sneutrino dark matter in the supersymmetric inverse seesaw models*, *JHEP* **02** (2014) 080 [[arXiv:1311.3497](#)] [[INSPIRE](#)].
- [71] J. Guo, Z. Kang, J. Li, T. Li and Y. Liu, *Simplified Supersymmetry with Sneutrino LSP at 8 TeV LHC*, [arXiv:1312.2821](#) [[INSPIRE](#)].
- [72] V. De Romeri and M. Hirsch, *Sneutrino Dark Matter in Low-scale Seesaw Scenarios*, *JHEP* **12** (2012) 106 [[arXiv:1209.3891](#)] [[INSPIRE](#)].
- [73] R. Kitano and K.-y. Oda, *Neutrino masses in the supersymmetric standard model with right-handed neutrinos and spontaneous R-parity violation*, *Phys. Rev. D* **61** (2000) 113001 [[hep-ph/9911327](#)] [[INSPIRE](#)].
- [74] D. Das and S. Roy, *One-loop contribution to the neutrino mass matrix in NMSSM with right-handed neutrinos and tri-bimaximal mixing*, *Phys. Rev. D* **82** (2010) 035002 [[arXiv:1003.4381](#)] [[INSPIRE](#)].
- [75] D.G. Cerdeno, C. Muñoz and O. Seto, *Right-handed sneutrino as thermal dark matter*, *Phys. Rev. D* **79** (2009) 023510 [[arXiv:0807.3029](#)] [[INSPIRE](#)].
- [76] D.G. Cerdeno and O. Seto, *Right-handed sneutrino dark matter in the NMSSM*, *JCAP* **08** (2009) 032 [[arXiv:0903.4677](#)] [[INSPIRE](#)].
- [77] D.G. Cerdeno, J.-H. Huh, M. Peiro and O. Seto, *Very light right-handed sneutrino dark matter in the NMSSM*, *JCAP* **11** (2011) 027 [[arXiv:1108.0978](#)] [[INSPIRE](#)].
- [78] K. Huitu, J. Laamanen, L. Leinonen, S.K. Rai and T. Ruppel, *Comparison of neutralino and sneutrino dark matter in a model with spontaneous CP-violation*, *JHEP* **11** (2012) 129 [[arXiv:1209.6302](#)] [[INSPIRE](#)].
- [79] P. Gondolo and G. Gelmini, *Cosmic abundances of stable particles: Improved analysis*, *Nucl. Phys. B* **360** (1991) 145.
- [80] M. Ibe, H. Murayama and T.T. Yanagida, *Breit-Wigner Enhancement of Dark Matter Annihilation*, *Phys. Rev. D* **79** (2009) 095009 [[arXiv:0812.0072](#)] [[INSPIRE](#)].
- [81] W.-L. Guo and Y.-L. Wu, *Enhancement of Dark Matter Annihilation via Breit-Wigner Resonance*, *Phys. Rev. D* **79** (2009) 055012 [[arXiv:0901.1450](#)] [[INSPIRE](#)].
- [82] G. Bélanger, F. Boudjema, A. Pukhov and A. Semenov, *MicrOMEGAS 2.0: A Program to calculate the relic density of dark matter in a generic model*, *Comput. Phys. Commun.* **176** (2007) 367 [[hep-ph/0607059](#)] [[INSPIRE](#)].

- [83] G. Bélanger, F. Boudjema, A. Pukhov and A. Semenov, *Dark matter direct detection rate in a generic model with MicrOMEGAs 2.2*, *Comput. Phys. Commun.* **180** (2009) 747 [[arXiv:0803.2360](#)] [[INSPIRE](#)].
- [84] G. Bélanger, F. Boudjema, A. Pukhov and A. Semenov, *MicrOMEGAs₃: A program for calculating dark matter observables*, *Comput. Phys. Commun.* **185** (2014) 960 [[arXiv:1305.0237](#)] [[INSPIRE](#)].
- [85] LAT collaboration, M. Ackermann et al., *Fermi LAT Search for Dark Matter in Gamma-ray Lines and the Inclusive Photon Spectrum*, *Phys. Rev. D* **86** (2012) 022002 [[arXiv:1205.2739](#)] [[INSPIRE](#)].
- [86] FERMI-LAT collaboration, M. Ackermann et al., *Constraining Dark Matter Models from a Combined Analysis of Milky Way Satellites with the Fermi Large Area Telescope*, *Phys. Rev. Lett.* **107** (2011) 241302 [[arXiv:1108.3546](#)] [[INSPIRE](#)].
- [87] PAMELA collaboration, O. Adriani et al., *PAMELA results on the cosmic-ray antiproton flux from 60 MeV to 180 GeV in kinetic energy*, *Phys. Rev. Lett.* **105** (2010) 121101 [[arXiv:1007.0821](#)] [[INSPIRE](#)].
- [88] F. Staub, *From Superpotential to Model Files for FeynArts and CalcHep/CompHEP*, *Comput. Phys. Commun.* **181** (2010) 1077 [[arXiv:0909.2863](#)] [[INSPIRE](#)].
- [89] F. Staub, T. Ohl, W. Porod and C. Speckner, *A Tool Box for Implementing Supersymmetric Models*, *Comput. Phys. Commun.* **183** (2012) 2165 [[arXiv:1109.5147](#)] [[INSPIRE](#)].
- [90] F. Staub, *SARAH 3.2: Dirac Gauginos, UFO output and more*, *Computer Physics Communications* **184** (2013) pp. 1792–1809 [[arXiv:1207.0906](#)] [[INSPIRE](#)].
- [91] W. Porod, *SPheno, a program for calculating supersymmetric spectra, SUSY particle decays and SUSY particle production at e^+e^- colliders*, *Comput. Phys. Commun.* **153** (2003) 275 [[hep-ph/0301101](#)] [[INSPIRE](#)].
- [92] W. Porod and F. Staub, *SPheno 3.1: Extensions including flavour, CP-phases and models beyond the MSSM*, *Comput. Phys. Commun.* **183** (2012) 2458 [[arXiv:1104.1573](#)] [[INSPIRE](#)].
- [93] A. Belyaev, N.D. Christensen and A. Pukhov, *CalcHEP 3.4 for collider physics within and beyond the Standard Model*, *Comput. Phys. Commun.* **184** (2013) 1729 [[arXiv:1207.6082](#)] [[INSPIRE](#)].
- [94] Y. Grossman and H.E. Haber, *Sneutrino mixing phenomena*, *Phys. Rev. Lett.* **78** (1997) 3438 [[hep-ph/9702421](#)] [[INSPIRE](#)].
- [95] T. Falk, K.A. Olive and M. Srednicki, *Heavy sneutrinos as dark matter*, *Phys. Lett. B* **339** (1994) 248 [[hep-ph/9409270](#)] [[INSPIRE](#)].